Functionalization of Liquid-Exfoliated Two-Dimensional 2H-MoS₂**

Claudia Backes, Nina C. Berner, Xin Chen, Paul Lafargue, Pierre LaPlace, Mark Freeley, Georg S. Duesberg, Jonathan N. Coleman, and Aidan R. McDonald*

Abstract: *Layered two-dimensional (2D) inorganic transition-metal dichalchogenides (TMDs) have attracted great interest as a result of their potential application in optoelectronics, catalysis, and medicine. However, methods to functionalize and process such 2D TMDs remain scarce. We have established a facile route towards functionalized layered MoS_2. We found that the reaction of liquid-exfoliated 2D MoS_2, with $M(OAc)_2$ salts (M = Ni, Cu, Zn; OAc = acetate) yielded functionalized MoS_2–$M(OAc)_2$ materials. Importantly, this method furnished the 2H-polytype of MoS_2 which is a semiconductor. X-ray photoelectron spectroscopy (XPS), diffuse reflectance infrared Fourier transform spectroscopy (DRIFT–IR), and thermogravimetric analysis (TGA) provide strong evidence for the coordination of MoS_2 surface sulfur atoms to the $M(OAc)_2$ salt. Interestingly, functionalization of 2H-MoS_2 allows for its dispersion/processing in more conventional laboratory solvents.*

Layered two-dimensional (2D) inorganic transition-metal dichalchogenides (TMDs) have recently received growing attention[1] mainly as a result of their potential application in optoelectronics, catalysis, electrochemistry, and medicine.[1,2] While significant progress has been made on the production of ultra-thin, high-quality TMDs by chemical vapor deposition (CVD) growth,[3] chemical exfoliation,[1b,4] or direct exfoliation in suitable solvents,[1c,5] reports on the functionalization of 2D TMDs remain scarce, limiting their further application. Functionalization of nanomaterials is critical for tailoring their surface properties to specific solvents/environments, enhancing their processability, and modulating their

conductivity. Even though 2D TMDs show good dispersibility in certain solvents, such as *N*-methyl-2-pyrrolidone (NMP), their dispersibility, and thus processibility, falls short in common laboratory solvents. To date, TMDs have proven difficult to functionalize because of their relative inertness. We set out to investigate a route towards functionalized TMDs.

As a model 2D TMD, we have focused our attention on MoS_2. We have recently reported methods for the facile preparation and extensive characterization of exfoliated MoS_2.[5,6] 2D MoS_2 has primarily been isolated in two polytypes, 2H-MoS_2 and 1T-MoS_2.[1b] In 2H-MoS_2 the Mo atom sits in a trigonal prismatic environment, whereas in 1T-MoS_2 the Mo atom sits in an octahedral environment. Critically, the polytypes display disparate electronic properties: thin-layered 2H-MoS_2 is a semiconductor (energy gap ≈ 1.2 eV) and a strong luminophore, whereas 1T-MoS_2 is conducting (metallic) and is not photoluminescent.[4,7] The structural and electronic properties of 1T-MoS_2 are poorly understood whereas in contrast those of 2H-MoS_2 are well established.[1,2] While a number of reports describing the covalent functionalization of MoS_2 have recently appeared,[8] all have employed a chemical exfoliation (ce) procedure that yields functionalized ce-1T-MoS_2.[4,7] This procedure entailed a harsh *tert*-butyllithium-mediated reduction of 2H-MoS_2 followed by oxidation and exfoliation of the resulting Li_xMoS_2 to yield ce-1T-MoS_2 nanosheets. To our knowledge, no methods for the functionalization of pristine 2D 2H-MoS_2 exist. Herein, we address this deficiency.

To functionalize 2H-MoS_2 in a mild and efficient manner, we have employed similar liquid exfoliation techniques to those reported recently (Figure 1).[1c,5,6,9] Rather than using the standard dispersion/exfoliation solvents, we used 2-propanol (IPA). Typically for 2H-MoS_2 exfoliation, NMP and *N*-cyclohexyl-2-pyrrolidone (CHP) are used because of the matching solubility parameters of solvent and solute.[1c,5,6b,9] We found these solvents unsuitable because: a) they tend to leave a residue on the surface of the 2H-MoS_2 that inhibited functionalization, b) their high boiling point prevented efficient drying and characterization of the material, and c) NMP has been identified as a reproductive

[*] Dr. C. Backes,[+] Dr. N. C. Berner,[+] X. Chen, P. Lafargue, P. LaPlace,
    M. Freeley, Prof. G. S. Duesberg, Prof. J. N. Coleman,
    Dr. A. R. McDonald
    CRANN/AMBER Nanoscience Institute
    Trinity College Dublin (TCD)
    College Green, Dublin 2 (Ireland)
    E-mail: aidan.mcdonald@tcd.ie

    Dr. N. C. Berner,[+] X. Chen, P. Lafargue, P. LaPlace, M. Freeley,
    Prof. G. S. Duesberg, Dr. A. R. McDonald
    School of Chemistry, TCD

    Dr. C. Backes,[+] Prof. J. N. Coleman
    School of Physics, TCD

[+] These authors contributed equally to this work.

Supporting information for this article is available on the WWW under http://dx.doi.org/10.1002/anie.201409412.

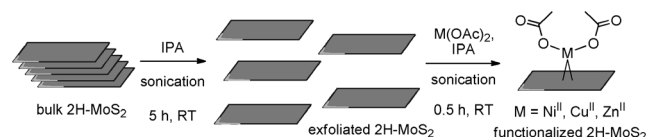***Figure 1.*** Schematic representation of the procedure for exfoliation and functionalization of 2H-MoS_2 nanosheets (IPA = 2-propanol, $M(OAc)_2$ = metal acetate salts).

toxin. Prior to functionalization, commercially available 2H-MoS$_2$ was initially sonicated in IPA for 5 hours (see the Supporting Information). Subsequent isolation of the exfoliated 2H-MoS$_2$ was achieved by centrifugation to remove unexfoliated material. As evidenced by atomic force microscopy (AFM, Figure 2), the 2H-MoS$_2$ material has been
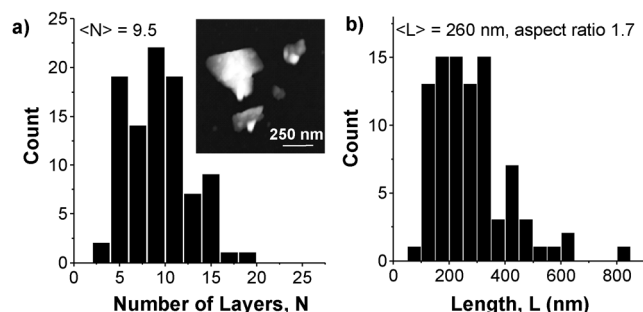

Figure 2. a) Thickness and b) length histograms compiled from atomic force microscopy after drop-casting a 2H-MoS$_2$ dispersion onto Si/SiO$_2$ wafers. Inset in (a): representative AFM image.

successfully exfoliated in IPA. AFM length and thickness analysis on a number of nanosheets was used to determine the mean lateral dimension < L > (260 nm) and degree of exfoliation < N > (9–10 layers) of the IPA-exfoliated 2H-MoS$_2$. Even though the concentration of exfoliated 2H-MoS$_2$ was typically lower by a factor of three compared to NMP,[5] IPA was found to be a suitable solvent, eliminating the problems associated with NMP/CHP.

The IPA-exfoliated 2H-MoS$_2$ was reacted with a variety of M(OAc)$_2$ salts. We postulated that surface sulfur atoms of the exfoliated 2H-MoS$_2$ would coordinate to the M(OAc)$_2$ salts, providing a facile route to functionalized 2H-MoS$_2$. The metal cations were anticipated to act as an anchor for (functional) organic carboxylate ligands to bind. Tremel and co-workers have taken a similar approach for the functionalization of TMD nanoparticles.[10] M(OAc)$_2$ salts (M = Cu, Ni, Zn) were dissolved in IPA (10 mM) and subsequently reacted with IPA-exfoliated 2H-MoS$_2$ (approximately 0.2 mM, v/v = 1) under tip sonication for 30 minutes. M(OAc)$_2$ salts were identified as suitable functionalities for two reasons: a) they display solubility in a variety of common laboratory solvents, such as acetone, alcohols, and nitriles (in contrast, metal halides do not); and b) they represent a large cohort of metal-carboxylate salts, where the carboxylate ligand can be easily derivatized allowing a broad scope of functional carboxylate group be tethered to the 2H-MoS$_2$ surface. A first indication of successful functionalization was provided through analysis of the optical extinction spectra of the functionalized materials. Upon functionalization, we noted marked changes in the concentration of 2H-MoS$_2$ dispersed in the IPA reaction mixture (as evidenced by changes in optical extinction intensity), indicating the dispersion properties of the 2H-MoS$_2$ had been altered. For 2H-MoS$_2$–Cu(OAc)$_2$ and 2H-MoS$_2$–Zn(OAc)$_2$ the concentration of dispersed 2H-MoS$_2$ decreased over 48 hours, suggesting partial reaggregation of the layered material. In contrast, 2H-MoS$_2$–Ni(OAc)$_2$ did not

display any reaggregation of exfoliated 2H-MoS$_2$, and in fact yielded more stable 2H-MoS$_2$ (see Figure S2 in the Supporting Information).

Critically, functionalization caused no changes in the relative intensities or energies of the optical excitation bands attributed to exfoliated 2H-MoS$_2$. This is very important, as it establishes that functionalization did not yield the 1T-polytype (1T-MoS$_2$ has an extinction spectrum very different to that of 2H-MoS$_2$).[4,6d] All other functionalization techniques to date have yielded 1T-MoS$_2$.[4,8]

Further proof of successful functionalization was obtained through analysis of the post-reaction supernatant solutions (where all functionalized 2H-MoS$_2$ has been removed). Cu(OAc)$_2$ displays a unique electronic absorption feature ($\lambda_{max} = 700$ nm) allowing us to monitor the uptake of the Cu^{II} salt by exfoliated 2H-MoS$_2$. A significant decrease in the $\lambda_{max} = 700$ nm feature assigned to Cu(OAc)$_2$ after functionalization was detected in the supernatant solutions, providing further strong evidence of the uptake of M(OAc)$_2$ salts by 2H-MoS$_2$. In summary, optical extinction spectroscopy provides encouraging evidence that functionalization of 2H-MoS$_2$ can be achieved through simple coordination chemistry.

Unequivocal evidence for the coordination of surface 2H-MoS$_2$ sulfur atoms to the metal atoms of the M(OAc)$_2$ salts was obtained using X-ray photoelectron spectroscopy (XPS). Survey spectra (Table S1) of the material confirmed the presence of surface Mo, S, M (Cu, Ni, Zn), C, and O atoms consistent with the functionalization of 2H-MoS$_2$ by M(OAc)$_2$ salts. Significantly, in all fitted XPS S 2p core level spectra (Figure 3 and Figure S5) a second well-separated component in the S 2p core level spectra at higher binding energies was clearly discernible in the functionalized materials. This is consistent with a proportion of surface sulfur atoms being found in a different chemical environment compared to the unfunctionalized material (Figure S4). As a result of coordination to the Lewis acidic metal atoms, the surface S-atom donors become more electropositive, resulting in a higher photoelectron emission energy. Analysis of the same spectra allowed us to estimate the degree of functionalization of the 2H-MoS$_2$ surface (see the Supporting Information). The ratio of the integrated peak intensity of the high-energy S 2p component to the total integrated S 2p core level peak yields a degree of surface functionalization of 50% in the case of 2H-MoS$_2$–Cu(OAc)$_2$, that is, 50% of the S atoms on the surface bear a functional group. For 2H-MoS$_2$–Ni(OAc)$_2$, and 2H-MoS$_2$–Zn(OAc)$_2$ values of 30% and 10% high-energy S 2p component, respectively, were determined. This pronounced difference in the degree of functionalization is not unexpected. The biding affinity of Cu, Ni, and Zn towards thioether ligands (analogous to S donors of 2H-MoS$_2$) tends to follow the trend Cu $\gg$ Ni > Zn.[12] We note that the successful chemical functionalization is also reflected in the Mo 3d core level XPS spectra (Figure S3). These spectra are complex (many overlapping components), however rough estimation of the degree of functionalization agrees very well with the values determined using the S 2p core spectra (Table S1). It should also be noted that the XPS survey indicated the presence of physisorbed M(OAc)$_2$, which comes from inefficient cleaning of the XPS samples (see the
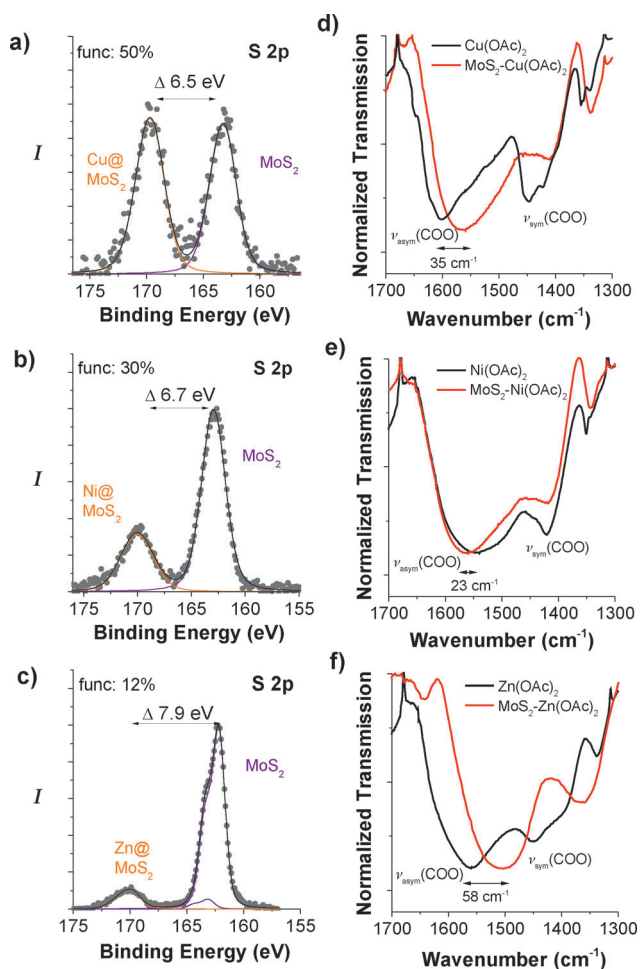
a)

b)

c)

d)

e)

f)

Figure 3. a–c) Fitted XPS S 2p core level spectra[11] of the 2H-MoS$_2$–M(OAc)$_2$ materials and d–f) DRIFT spectra of the M(OAc)$_2$ salts and 2H-MoS$_2$–M(OAc)$_2$ compounds. M = Cu (a, d); M = Ni (b, e); M = Zn (c, f).

Supporting Information). Overall, XPS analysis has allowed us to establish a direct sulfur–metal interaction in 2H-MoS$_2$–M(OAc)$_2$.

The high degree of functionalization clearly demonstrates that the M(OAc)$_2$ functionalities are binding to the basal plane of the 2D 2H-MoS$_2$. If the M(OAc)$_2$ functionalities were reacting only at disulfide-rich edge sites,[13] the degree of functionalization would be expected to be considerably lower. We can estimate the ratio of edge to basal plane sites by modeling the 2H-MoS$_2$ nanosheets as rectangles with a mean length of 260 nm and a mean width of 150 nm (from AFM, Figure 2). The perimeter (edge sites, 820 nm × 1 nm) constitutes roughly 2% of the sites that are present in the basal plane (39 000 nm^2), consequently yielding a maximum degree of edge functionalization of 2%. This is an encouraging outcome, given that analysis of the XPS-determined values for the degree of surface functionalization would suggest that 50% of surface S atoms in 2H-MoS$_2$–Cu(OAc)$_2$ coordinates to a Cu atom. To address further how the M(OAc)$_2$ salts are reacting with the 2H-MoS$_2$, we attempted to defunctionalize the materials by washing with a coordinating solvent. Extensive washing and sonication of 2H-MoS$_2$–Cu(OAc)$_2$ in

NMP resulted in the complete defunctionalization of the material. XPS analysis of the defunctionalized material yielded spectra identical to those of pristine 2H-MoS$_2$ (Figure S5). Furthermore, negligible changes in the zeta potential of 2H-MoS$_2$–Cu(OAc)$_2$ compared to pristine 2H-MoS$_2$ were detected (Figure S6). These combined results demonstrate that M(OAc)$_2$ salts are not binding at sulfur vacancies, are not causing sulfur vacancies to appear (by eliminating S atoms), and are not causing irreversible oxidation of the parent 2H-MoS$_2$.

To understand further the 2H-MoS$_2$–M(OAc)$_2$ interaction, we employed diffuse reflectance infrared Fourier transform (DRIFT) spectroscopy, which provided proof of a direct 2H-MoS$_2$/M(OAc)$_2$ interaction (Figure 3 and Figures S7 and 8). The sharp feature detected at 383 cm^{-1} is typical of 2H-MoS$_2$.[14] For all of the functionalized materials, the presence of the acetate ligands is clearly evidenced by the characteristic $\nu_{C=O}$ (1550–1600 cm^{-1}) of the metal-bound acetate ligand.[15] Significantly, in the functionalized materials, the $\nu_{C=O}$ associated with the acetate ligands were shifted by between 20 and 60 cm^{-1} when compared to the parent M(OAc)$_2$ salts. This shift provides a strong indication of a change in the coordination environment at the metal center of the acetate salt, presumably as a result of ligation by the S donors of the 2H-MoS$_2$ to the metal ion. An analysis of 2H-MoS$_2$–Cu(OAc)$_2$ provides further insight. In the solid state, Cu(OAc)$_2$ is a dimeric species containing two Cu atoms bridged by four acetate ligands ([Cu$_2$(OAc)$_4$]). The $\nu_{C=O}$ in 2H-MoS$_2$–Cu(OAc)$_2$ (1565 cm^{-1}) is typical of a species containing end-on binding acetate ligands (and not bridging acetates which have a typical $\nu_{C=O} \approx 1600$ cm^{-1}).[16] These observations suggest the metal has been ligated by surface S atoms causing the dimeric [Cu$_2$(OAc)$_4$] to break up, resulting in the formation of 2H-MoS$_2$–Cu(OAc)$_2$ with end-on binding acetate ligands. In summary, the pronounced shifts of the $\nu_{C=O}$ mode of the metal-bound acetate ligands strongly suggests an interaction between the metal centers and the sulfur atoms of the 2H-MoS$_2$.

Thermogravimetric analysis (TGA) provided further proof of successful functionalization of 2H-MoS$_2$. Between 50°C and 400°C, the parent 2H-MoS$_2$ displayed negligible weight loss. In contrast, 2H-MoS$_2$–Cu(OAc)$_2$ displayed a significant (15%) and very sharp weight loss at approximately 200°C, indicative of the loss of organic surface functionalities (Figure S9). In support of this, DRIFT–IR analysis of the post-TGA 2H-MoS$_2$–Cu(OAc)$_2$ sample showed the disappearance of all $\nu_{C=O}$ features that were attributed to surface-bound acetate groups (Figure S10). Raman spectroscopy showed that the material after TGA was predominantly 2H-MoS$_2$ (Figure S11). These results would suggest that the weight loss at approximately 200°C is as a result of the thermal decomposition of the organic surface groups.

An important aspect to the functionalization of 2D nanomaterials is the alteration of the surface properties of the material as a result of the attachment of functional moieties.[6a] To investigate the effects of the surface functionalities in 2H-MoS$_2$–M(OAc)$_2$, we have redispersed 2H-MoS$_2$–Cu(OAc)$_2$ in NMP, IPA, and acetone. We have used 2H-MoS$_2$–Cu(OAc)$_2$ because it showed the highest degree of

functionalization. We compared the dispersibility of 2H-MoS$_2$–Cu(OAc)$_2$ to an exfoliated 2H-MoS$_2$ reference material (Figure 4). The 2H-MoS$_2$ reference was dispersed well in NMP and showed a reasonable dispersibility in IPA. In acetone, no 2H-MoS$_2$ was stably dispersed. In contrast, the functionalized 2H-MoS$_2$–Cu(OAc)$_2$ could not be stably dispersed in NMP, was reasonably well dispersed in IPA, and displayed a significantly enhanced uptake in acetone.
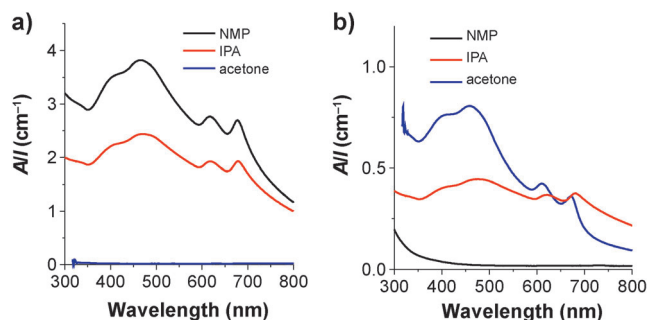

Figure 4. Optical extinction spectra of pre-sonicated a) 2H-MoS$_2$ reference powder and b) 2H-MoS$_2$–Cu(OAc)$_2$ after redispersion in NMP (black), IPA (red), and acetone (blue).

Nanomaterial dispersibility can be described reasonably well in the framework of Hansen solubility parameters.[5,17] To minimize the energetic cost of dispersion, the enthalpy of mixing needs to be minimized. This is the case when solubility parameters, namely δ_D (dispersive), δ_P (polar), and δ_H (hydrogen-bonding solubility parameter), of solvent and solute match (see the Supporting Information).[5,17] Using HSPiP (Hansen solubility parameters in practice, Y-MB algorithm) software, we can estimate the solubility parameters of the acetate ligands to be $\delta_D = 14.7$ MPa$^{1/2}$, $\delta_P = 12.5$ MPa$^{1/2}$, and $\delta_H = 7.9$ MPa$^{1/2}$, respectively. Although polar and H-bonding Hansen solubility parameters are close to NMP, the dispersive component is significantly lower. It is thus expected that successful surface modification by functionalization would decrease the dispersibility in NMP. In our redispersion experiments, we found this to be true, as the concentration of "2H-MoS$_2$" (estimated from the optical extinction value at $\lambda = 345$ nm) was decreased by a factor of more than 40 in 2H-MoS$_2$–Cu(OAc)$_2$ compared to pristine 2H-MoS$_2$. In IPA ($\delta_D = 15.8$ MPa$^{1/2}$, $\delta_P = 6.1$ MPa$^{1/2}$, $\delta_H = 16.4$ MPa$^{1/2}$), the concentration of 2H-MoS$_2$–Cu(OAc)$_2$ was lower by a factor of 5 compared to the reference. As the solubility parameters of IPA neither perfectly match those of the acetate ligands nor the 2H-MoS$_2$, quantitative analysis of this behavior is challenging. All three solubility parameters of the acetate ligands are close to acetone ($\delta_D = 15.5$ MPa$^{1/2}$, $\delta_P = 10.4$ MPa$^{1/2}$, $\delta_H = 7$ MPa$^{1/2}$) so that an enhanced dispersibility of the functionalized 2H-MoS$_2$ is expected. We detected a 20-fold increase in concentration of 2H-MoS$_2$–Cu(OAc)$_2$ in acetone compared to the non-functionalized 2H-MoS$_2$ – consistent with expectations derived from Hansen solubility parameters. Overall, the introduction of M(OAc)$_2$ functionalities onto the surface of exfoliated 2H-MoS$_2$ has dramatically altered the dispersibility properties of the material, allowing for the surface tuning of the material to specific solvents.

In conclusion, we have demonstrated a facile route towards functionalized 2H-MoS$_2$. Until now, procedures for the preparation of functionalized exfoliated TMDs, such as MoS$_2$, have yielded the 1T polytype, which is metallic. We have shown that the reaction of liquid exfoliated 2H-MoS$_2$ (a semiconductor) with metal carboxylate salts yields functionalized 2H-MoS$_2$–M(OAc)$_2$. Functionalization was achieved through coordination of surface S atoms with the metal center of the metal carboxylate salts. XPS, DRIFT–IR, and TGA analysis provide strong support for this surface functionalization. Most interestingly, functionalization of the 2H-MoS$_2$ allows for its dispersion in nonconventional solvents including IPA and acetone. At present we are investigating a variety of copper(II) salts as functional groups on the surface of 2H-MoS$_2$. We expect functionalization of 2H-MoS$_2$ with Cu^{II} salts to facilitate dispersion of 2H-MoS$_2$ in solvents displaying a wide range of polarities (i.e. from water to aliphatic hydrocarbons).

[1] a) S. Z. Butler, S. M. Hollen, L. Cao, Y. Cui, J. A. Gupta, H. R. Gutierrez, T. F. Heinz, S. S. Hong, J. Huang, A. F. Ismach, E. Johnston-Halperin, M. Kuno, V. V. Plashnitsa, R. D. Robinson, R. S. Ruoff, S. Salahuddin, J. Shan, L. Shi, M. G. Spencer, M. Terrones, W. Windl, J. E. Goldberger, *ACS Nano* **2013**, *7*, 2898–2926; b) M. Chhowalla, H. S. Shin, G. Eda, L.-J. Li, K. P. Loh, H. Zhang, *Nat. Chem.* **2013**, *5*, 263–275; c) V. Nicolosi, M. Chhowalla, M. G. Kanatzidis, M. S. Strano, J. N. Coleman, *Science* **2013**, *340*, 1226419; d) M. Xu, T. Liang, M. Shi, H. Chen, *Chem. Rev.* **2013**, *113*, 3766–3798.

[2] Q. H. Wang, K. Kalantar-Zadeh, A. Kis, J. N. Coleman, M. S. Strano, *Nat. Nanotechnol.* **2012**, *7*, 699–712.

[3] a) Y. J. Zhan, Z. Liu, S. Najmaei, P. M. Ajayan, J. Lou, *Small* **2012**, *8*, 966–971; b) A. Berkdemir, H. R. Gutierrez, A. R. Botello-Mendez, N. Perea-Lopez, A. L. Elias, C.-I. Chia, B. Wang, V. H. Crespi, F. Lopez-Urias, J.-C. Charlier, H. Terrones, M. Terrones, *Sci. Rep.* **2013**, *3*, 1755.

[4] G. Eda, H. Yamaguchi, D. Voiry, T. Fujita, M. Chen, M. Chhowalla, *Nano Lett.* **2011**, *11*, 5111–5116.

[5] J. N. Coleman, M. Lotya, A. O'Neill, S. D. Bergin, P. J. King, U. Khan, K. Young, A. Gaucher, S. De, R. J. Smith, I. V. Shvets, S. K. Arora, G. Stanton, H.-Y. Kim, K. Lee, G. T. Kim, G. S. Duesberg, T. Hallam, J. J. Boland, J. J. Wang, J. F. Donegan, J. C. Grunlan, G. Moriarty, A. Shmeliov, R. J. Nicholls, J. M. Perkins, E. M. Grieveson, K. Theuwissen, D. W. McComb, P. D. Nellist, V. Nicolosi, *Science* **2011**, *331*, 568–571.

[6] a) G. Cunningham, M. Lotya, C. S. Cucinotta, S. Sanvito, S. D. Bergin, R. Menzel, M. S. P. Shaffer, J. N. Coleman, *ACS Nano* **2012**, *6*, 3468–3480; b) A. O'Neill, U. Khan, J. N. Coleman, *Chem. Mater.* **2012**, *24*, 2414–2421; c) K. R. Paton, E. Varrla, C. Backes, R. J. Smith, U. Khan, A. O'Neill, C. Boland, M. Lotya, O. M. Istrate, P. King, T. Higgins, S. Barwich, P. May, P. Puczkarski, I. Ahmed, M. Moebius, H. Pettersson, E. Long, J.

Coelho, S. E. O'Brien, E. K. McGuire, B. M. Sanchez, G. S. Duesberg, N. McEvoy, T. J. Pennycook, C. Downing, A. Crossley, V. Nicolosi, J. N. Coleman, *Nat. Mater.* **2014**, *13*, 624–630; d) C. Backes, R. J. Smith, N. McEvoy, N. C. Berner, D. McCloskey, H. C. Nerl, A. O'Neill, P. J. King, T. Higgins, D. Hanlon, N. Scheuschner, J. Maultzsch, L. Houben, G. S. Duesberg, J. F. Donegan, V. Nicolosi, J. N. Coleman, *Nat. Commun.* **2014**, *5*, 4576.

[7] a) F. Wypych, R. Schollhorn, *Chem. Commun.* **1992**, 1386–1388; b) E. Benavente, M. A. S. Ana, F. Mendizábal, G. González, *Coord. Chem. Rev.* **2002**, *224*, 87–109.

[8] a) S.-D. Jiang, G. Tang, Z.-M. Bai, Y.-Y. Wang, Y. Hu, L. Song, *RSC Adv.* **2014**, *4*, 3253–3262; b) S. S. Chou, M. De, J. Kim, S. Byun, C. Dykstra, J. Yu, J. Huang, V. P. Dravid, *J. Am. Chem. Soc.* **2013**, *135*, 4584–4587; c) L. Zhou, B. He, Y. Yang, Y. He, *RSC Adv.* **2014**, *4*, 32570–32578.

[9] a) Y. Hernandez, M. Lotya, D. Rickard, S. D. Bergin, J. N. Coleman, *Langmuir* **2010**, *26*, 3208–3213; b) S. Barwich, U. Khan, J. N. Coleman, *J. Phys. Chem. C* **2013**, *117*, 19212–19218; c) J. N. Coleman, *Acc. Chem. Res.* **2013**, *46*, 14–22; d) D. Hanlon, C. Backes, T. M. Higgins, M. Hughes, A. O'Neill, P. King, N. McEvoy, G. S. Duesberg, B. M. Sanchez, H. Pettersson, V. Nicolosi, J. N. Coleman, *Chem. Mater.* **2014**, *26*, 1751–1763.

[10] M. N. Tahir, N. Zink, M. Eberhardt, H. A. Therese, U. Kolb, P. Theato, W. Tremel, *Angew. Chem. Int. Ed.* **2006**, *45*, 4809–4815; *Angew. Chem.* **2006**, *118*, 4927–4933.

[11] The S component centered at 163 eV is attributed to S at the edges of the nanosheets, see Ref. [6d].

[12] S. G. Murray, F. R. Hartley, *Chem. Rev.* **1981**, *81*, 365–414.

[13] a) J. V. Lauritsen, M. V. Bollinger, E. Lægsgaard, K. W. Jacobsen, J. K. Nørskov, B. S. Clausen, H. Topsøe, F. Besenbacher, *J. Catal.* **2004**, *221*, 510–522; b) J. V. Lauritsen, J. Kibsgaard, S. Helveg, H. Topsoe, B. S. Clausen, E. Laegsgaard, F. Besenbacher, *Nat. Nanotechnol.* **2007**, *2*, 53–58; c) H. I. Karunadasa, E. Montalvo, Y. Sun, M. Majda, J. R. Long, C. J. Chang, *Science* **2012**, *335*, 698–702.

[14] T. J. Wieting, J. L. Verble, *Phys. Rev. B* **1971**, *3*, 4286–4292.

[15] Y. Mathey, D. R. Greig, D. F. Shriver, *Inorg. Chem.* **1982**, *21*, 3409–3413.

[16] G. B. Deacon, R. J. Phillips, *Coord. Chem. Rev.* **1980**, *33*, 227–250.

[17] a) J. N. Coleman, *Adv. Funct. Mater.* **2009**, *19*, 3680–3695; b) J. M. Hughes, D. Aherne, J. N. Coleman, *J. Appl. Polym. Sci.* **2013**, *127*, 4483–4491.